Journal of Applied Polymer Science

Synthesis of well-defined amphiphilic block copolymers via AGET ATRP used for hydrophilic modification of PVDF membrane

Haixiang Sun,[1,2] Tiantian Wang,[1] Yingying Zhou,[2] Peng Li,[2] Ying Kong[2]

[1]College of Science, China University of Petroleum (East China), Qingdao 266580, People's Republic of China

[2]State Key Laboratory of Heavy Oil Processing, China University of Petroleum (East China), Qingdao 266580, People's Republic of China

Correspondence to: H. Sun (E-mail: sunhaixiang@upc.edu.cn)

ABSTRACT: A well-defined amphiphilic block copolymer consisting of a hydrophobic block poly(methyl methacrylate) (PMMA) and a hydrophilic block poly[*N*,*N*–2-(dimethylamino) ethyl methacrylate] (PDMAEMA) was synthesized by activator generated by the electron transfer for atom transfer radical polymerization method (AGET ATRP). Kinetics study revealed a linear increase in the graph concentration of PMMA-*b*-PDMAEMA with the reaction time, indicating that the polymer chain growth was consistent with a controlled process. The gel permeation chromatography results indicated that the block copolymer had a narrow molecular weight distribution ($Mw/Mn = 1.42$) under the optimal reaction conditions. Then, poly(vinylidene fluoride) (PVDF)/PMMA-*b*-PDMAEMA blend membranes were prepared via the standard immersion precipitation phase inversion process, using the block copolymer as additive to improve the hydrophilicity of the PVDF membrane. The presence and dispersion of PMMA-*b*-PDMAEMA clearly affected the morphology and improved the hydrophilicity of the as-synthesized blend membranes as compared to the pristine PVDF membranes. By incorporating 15 wt % of the block copolymer, the water contact angle of the resulting blend membranes decreased from pure PVDF membrane 98° to 76°. The blend membranes showed good stability in the 20 d pure-water experiment. The bovine serum albumin (BSA) absorption experiment revealed a substantial antifouling property of the blend membranes in comparison with the pristine PVDF membrane. © 2015 Wiley Periodicals, Inc. J. Appl. Polym. Sci. **2015**, *132*, 42080.

KEYWORDS: blends; copolymers; structure-property relations; surfaces and interfaces; synthesis and processing

Received 20 October 2014; accepted 9 February 2015

DOI: 10.1002/app.42080

INTRODUCTION

Poly(vinylidene fluoride) (PVDF) is one of the most popular materials in chemical industry with excellent physical and chemical resistance, thermal stability, low toxicity, and low cost.[1,2] However, because of the low surface energy and strong hydrophobicity of PVDF matrix, it suffers from significant nonspecific protein adsorption on the membrane surface where PVDF membranes are applied, which often causes severe membrane fouling resulting in a rapid decline of permeation flux.[3–5] To improve the surface hydrophilicity of PVDF membranes, a large amount of work has been devoted to the surface modification of PVDF such as surface coating,[6] surface grafting,[7,8] UV photoirradiation,[9] blending modification,[10,11] and the incorporation of inorganic nanoparticles.[12,13] Blending modification is one of the most versatile approaches that can be applied to industrial-scale production. In this method, linear water-soluble polymers are used as the additives for the hydrophilization of PVDF membranes. However, because of the weak interaction between the additives and the polymer matrix, the additives tend to release from the membranes during long-term use. Therefore, the stability of the blending membranes remains an issue in practical applications.[14] The blending of amphiphilic polymers with PVDF is one of the popular methods for the hydrophilic modification of PVDF membranes.[15–17] The advantage of this method is that the amphiphilic copolymer additives can preferentially segregate on the surface of the membrane, thus increasing the long-term stability of the hydrophilic and antifouling layers on the PVDF membrane surface.

Traditionally, well-defined polymer architectures such as block copolymers have been synthesized by living polymerization techniques. The recent advances in controlled/"living" radical polymerization[18,19] have made it possible to synthesize controlled polymer architectures, usually only accessible by living ionic polymerization. Much progress in controlled radical polymerization has been made in terms of a better control of polymerization in nitroxide-mediated,[20] metal-mediated,[21] and atom transfer radical polymerization (ATRP).[22–24] ATRP has already been widely used for the synthesis of block, graft, and

star copolymers as well as polymers with more complex structures based on diverse monomers. However, normal ATRP suffers from the fact that the used catalyst is sensitive to air and other oxidants. The activator generated by electron transfer for atom transfer radical polymerization (AGET ATRP)[25,26] technology not only solves the problem of the storage of the catalyst, but also enables the polymerization to proceed with a low amount of catalyst in the presence of a certain amount of air. In a typical AGET ATRP system, a transition-metal complex in its higher oxidation state, for example Cu(II) complex, is used as the catalyst instead of Cu(I) complex used for the normal ATRP system, and a stoichiometric amount of a reducing agent such as ascorbic acid and Sn(II) 2-ethylhexanoate are introduced into the system. In recent years, AGET ATRP technology has been used to synthesize well-defined polymers and materials with complex architectures derived from all types of monomers such as *N*,*N*–2-(dimethylamino)ethyl methacrylate (DMAEMA),[27] styrene,[28] methacrylate,[29] and acrylate.[30] However, the synthesis of amphiphilic block copolymer with methyl methacrylate (MMA) and DMAEMA has rarely been reported.

In this study, a well-defined amphiphilic block copolymer poly(methyl methacrylate)-*b*-poly[*N*, *N*–2-(dimethylamino)ethyl methacrylate] (PMMA-*b*- PDMAEMA) was synthesized by the AGET ATRP method. MMA was selected as the hydrophobic monomer based on its excellent compatibility with PVDF and DMAEMA was selected as the hydrophilic monomer to improve the surface hydrophilicity of PVDF membranes. The chemical composition and molecular-weight distribution of PMMA and PMMA-*b*-PDMAEMA were determined by Fourier transform infrared spectroscopy (FTIR), ^{1}H-NMR and gel permeation chromatography (GPC). Then, PVDF/PMMA-*b*-PDMAEMA blend membranes were prepared via the immersion precipitation phase inversion process using the synthesized block copolymer as the additive. The morphology and hydrophilicity of the blend membrane surface containing different amounts of the block copolymer were characterized by scanning electron microscopy (SEM) and water contact angle. Finally, the pure water permeability and antifouling properties of the blend membranes were investigated by the dead-end filtration and protein bovine serum albumin (BSA) solution absorption experiments.

EXPERIMENTAL

Materials

The MMA (98 wt %, Shanghai Chemical Reagent) was purified by extracting with a 5 wt % sodium hydroxide (NaOH) aqueous solution, followed by washing with water, drying with anhydrous sodium sulfate (Na_2SO_4) overnight, and finally distilling under vacuum. The DMAEMA (98 wt %, Shanghai Chemical Reagent) was purified by passing through a column of basic alumina to remove the stabilizing agent and distilling over calcium hydride (CaH_2) prior to use. PVDF ($M_n = 2.0 \times 10^5$) was obtained from Shanghai 3F New Materials and dried at 110°C for at least 12 h to remove the water prior to use. BSA ($M_n = 67$ kDa, pI = 4.7) was purchased from Fluka (Switzerland). Copper bromide ($CuBr_2$), ethyl 2-bromoisobutyrate (EBiB), *N*,*N*,*N*,*N*,*N*-pentamethyldiethylenetriamine (PMDETA), and vitamin C (VC) were purchased from Sinopharm Chemical Reagent. *N*,*N*-dimethylformamide (DMF) and tetrahydrofuran (THF) were used as received without further purification.

Synthesis of Amphiphilic Block Copolymer PMMA-*b*-PDMAEMA

PMMA with bromine as the radical transferable group was synthesized by AGET ATRP using EBiB as the initiator and $CuBr_2$ and VC complexed by PMDETA as the catalyst in 50 vol % anisole. The role of VC in the system is to reduce the Cu (II) into Cu(I) as catalyst instead of adding Cu (I) complex at the beginning, which overcomes the sensitive problem of the catalyst Cu(I) in the presence of a certain amount of air. A typical polymerization procedure for the molar ratio of $[MMA]_0/[EBiB]_0/[CuBr_2]_0/[PMDETA]_0/[VC]_0 = 200 : 1 : 1 : 2 : 1$ was as follows: First, 0.15 mol MMA was dissolved in 40 mL DMF; then, 0.75 mmol EBiB initiator, 0.75 mmol $CuBr_2$ and 1.5 mmol PMDETA were added to a dried three-neck flask, which was thoroughly bubbled with N_2 for 20 min to eliminate the dissolved oxygen in the mixture. For the deoxygenated system, a bubbled solution of 0.75 mmol VC in 1 mL DMF was added; then, the three-neck flask was sealed and transferred to an oil bath held by a thermostat at the desired temperature of 90°C to polymerize for 12 h under stirring. After the desired polymerization time, the three-neck flask was cooled by immersing in an ice-water bath. Then, the flask was opened, and the contents were dissolved in THF (~2 mL) and precipitated using a large amount of acetone (~200 mL). The polymer obtained by filtration was dried under vacuum until a constant weight at 60°C. The monomer conversion was determined gravimetrically.

The amphiphilic block copolymer, PMMA-*b*-PDMAEMA, was synthesized by AGET ATRP using well-defined PMMA-Br as the macroinitiator and $CuBr_2$ and VC complexed by PMDETA as the catalyst in 50 vol % anisole. The molar ratio of $[DMAEMA]_0/[PMMA\text{-}Br]_0/[CuBr_2]_0/[PMDETA]_0/[VC]_0$ was 200 : 1 : 1 : 2 : 1, and the procedure was the same as the synthesis of PMMA. The synthetic procedure for the amphiphilic block copolymer was shown in Figure 1. The final product was characterized by ^{1}H NMR and GPC. The products were synthesized more than twice to make sure the reproducibility of the experimental results.

Preparation of Pure PVDF and PVDF/PMMA-*b*-PDMAEMA Blend Membranes

The pure PVDF and PVDF/PMMA-*b*-PDMAEMA blend membranes were fabricated by the phase inversion method. The casting solution was prepared using a certain amount of PVDF polymer dissolved in DMF at 70°C and filtered to remove undissolved materials and dust particles. After degassing, the homogeneous PVDF solution was cast onto the surface of a nonwoven fabric of area 120 × 160 mm^2, using a scraper with a 0.2 mm gap at ambient temperature (24°C) and humidity (53–54%); then, the solution was immediately immersed into a coagulation bath of water at 20°C to form pure PVDF membranes. The pure membranes were washed thoroughly with deionized water to remove residual solvent and stored in fresh deionized water for further use.

The PVDF/PMMA-*b*-PDMAEMA blend membranes were synthesized in the same manner as the pure PVDF membranes

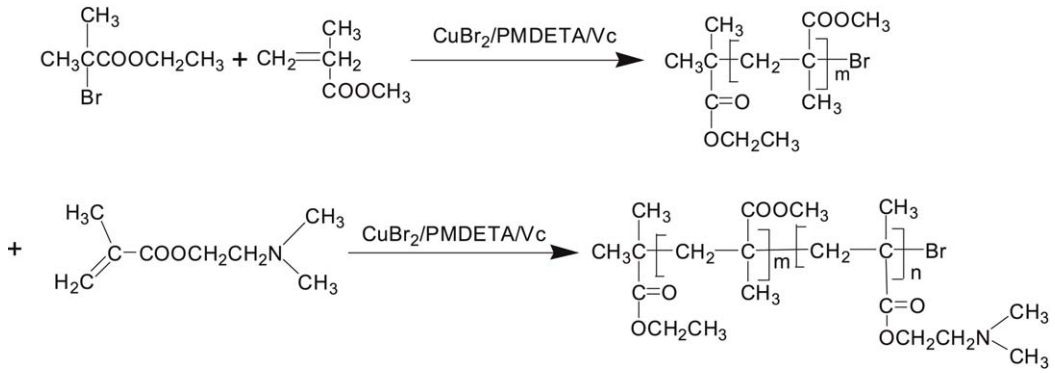

Figure 1. Synthetic procedure of amphiphilic block copolymers by AGET ATRP.

except that an amount of PMMA-*b*-PDMAEMA was added to the casting solution under vigorous stirring after the polymer had completely dissolved. The components of the casting solution were listed in Table I. Moreover, ultrasonic vibration was used to ensure that PMMA-*b*-PDMAEMA was evenly dispersed in the casting solution, which was later kept in darkness for more than 24 h to eliminate the bubbles.

Characterization and Measurements

The FTIR characterizations of PMMA and PMMA-*b*-PDMAEMA were performed with a 170SX FTIR spectroscopy (Nicolet, US). The measured wavenumber range was between 4000 and 400 cm^{-1} at a resolution of 4 cm^{-1}. All original spectra were baseline corrected using the Omnic 6.1 software. The ^1H NMR spectra were measured using a Bruker AC-600 instrument at room temperature with $CDCl_3$ as the solvent and tetramethylsilane (TMS) as the internal standard.

The molecular weights and polydispersity index (M_w/M_n, PDI) of PMMA and PMMA-*b*-PDMAEMA polymers were measured using GPC system (Viscotek M302 TDA, USA), and THF was used as the eluent with a flow rate of 1.0 mL/min at 40°C.

The top surface and cross-section morphology of the pure PVDF and blend membranes were observed by SEM (S-4800, Hitachi, Japan) after coating with a conductive layer of sputtered gold. The cross section was obtained by snap-freezing the membranes in liquid nitrogen.

The tendency of water droplets to spread on the membrane surface is directly affected by its hydrophilicity. In this way, very small droplets of the deionized water were dropped on the membranes surface in several random places, and the imaging of droplets was taken by use of a water contact angle system (KINO Industry, USA) equipped with video capture at room temperature. To minimize the experimental error, the contact water angles were measured at least five times for each sample and then averaged.

Table I. Composition of Casting Solution for PVDF/PMMA-*b*-PDMAEMA Blend Membranes Preparation

Membrane	PMMA-*b*-PDMAEMA (g)	PVDF (g)	DMF (mL)
Pure PVDF	0	15.00	85
5 wt % M-D/PVDF	0.75	14.25	85
7 wt % M-D/PVDF	1.05	13.95	85
10 wt % M-D/PVDF	1.50	13.50	85
12 wt % M-D/PVDF	1.80	13.20	85
15 wt % M-D/PVDF	2.25	12.75	85

Filtration experiments were carried out on the membranes with a diameter of 30 mm using a dead-end stirred filtration cell. Under a pressure of 100 kPa and a feed temperature of 25 ± 0.1°C, the flux of pure water (J_w) was obtained from the volume of the permeated water within 30 min and calculated as follows:

$$J_w = \frac{Q}{A \times \Delta t} \quad (1)$$

where J_w is the pure water flux (L/(m^2 h)), Q is the permeate volume (L), A is the membrane area (m^2), and Δt is the time (h).

BSA, as a model protein, was used to investigate the adsorption of protein on the blend membranes by the batchwise method. The membranes (9 cm^2) were washed and equilibrated by shaking in a 20 m*M* sodium phosphate buffer, pH 7.4 with 0.15*M* NaCl for 2 h. Then, the membranes were shaken in 2 mL of BSA solutions with different concentrations from 0.2 to 0.8 mg/mL for one day at 25°C. The pH values of the solutions were adjusted to 4.5 by adding a small amount of 0.1*M* HCl and the ionic strength was adjusted to 0.2*M* with NaCl. The concentrations of BSA in the solutions were measured using an S-54 UV–visible spectrometer (Shanghai Lengguang Tech) at 595 nm according to the Bradford method.[31] The amount of BSA adsorption was calculated from the difference between the concentrations before and after the adsorption. The adsorption isotherm was plotted as the adsorption capacity versus the equilibrated concentration of BSA in the solution.

Membrane fouling curtails severely the economical and practical implementation of the membrane process. To investigate the fouling resistance of the prepared blend membrane, 1 g/L BSA as a model protein solution permeation process was conducted in this study. Under the pressure of 150 kPa at room temperature, the membrane was pre-pressured about 30 min. Then, the water permeate flux (J_p) was obtained after the filtration of BAS

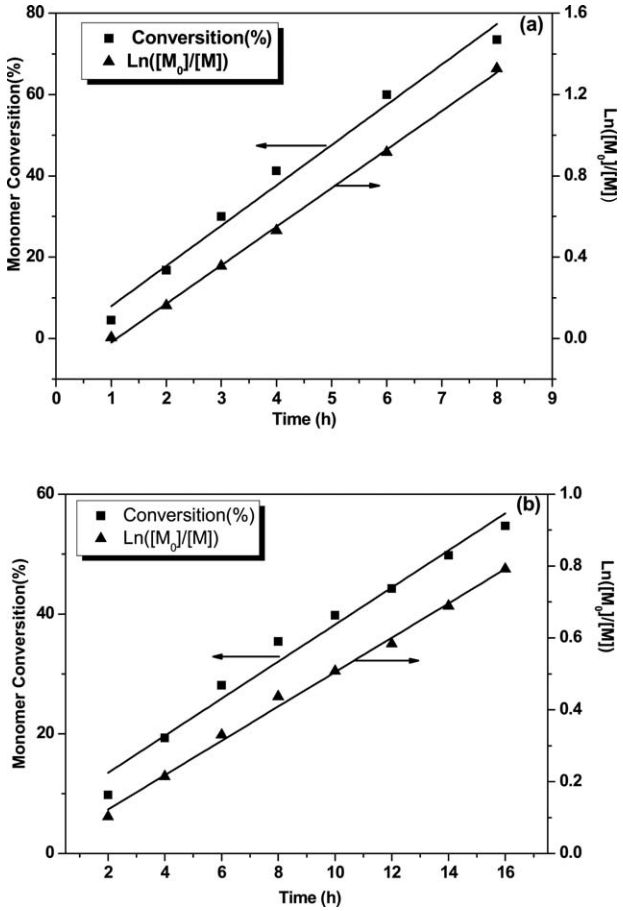

Figure 2. ln([M_0]/[M]) and monomer conversion as a function of time for AGET ATRP of PMMA (a) and PMMA-*b*-PDMAEMA, (b) in the presence of air at 90°C.

solution at 100 kPa. After filtration of BSA solution, the membrane was cleaned via pure water for three times and then the pure water flux (J_r) was measured again. According to the eq. (1), the flux of pure water J_w was obtained. By comparing the value of J_w, J_p, and J_r, the water flux reduction and the cleaning property of the fouled membrane were investigated. The filtration experiments were measured five times and then averaged. The water flux reduction (*FR*) was calculated as follows:[32]

$$\mathrm{FR}(\%) = \frac{J_w - J_p}{J_w} \times 100\% \quad (2)$$

The reversible fouling index (*RFI*) was obtained from the eq. (3).

$$\mathrm{RFI} = \frac{J_w - J_r}{J_w} \quad (3)$$

RESULTS AND DISCUSSION

Characterization of PMMA and PMMA-*b*-PDMAEMA

Kinetic Study. To further confirm the nature of the "living"/controlled radical polymerization of AGET ATRP, PMMA-Br was used as the macroinitiators for further polymerization of fresh monomers DMAEMA. Block copolymerization of PDMAEMA was also carried out using the catalyst system mentioned above in the presence of oxygen. The amphiphilic block

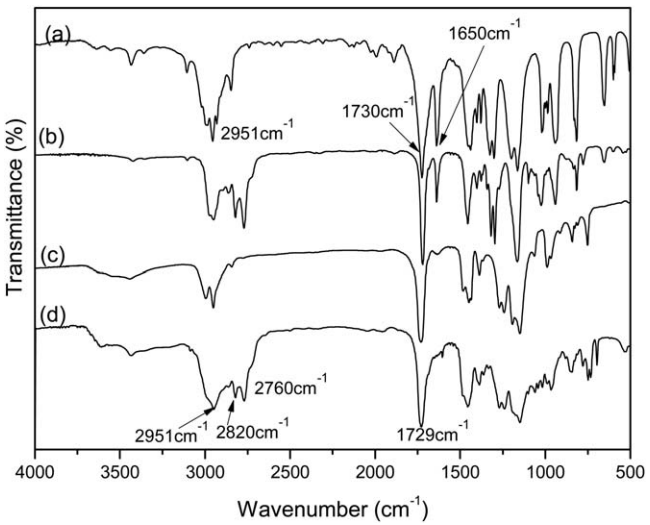

Figure 3. FTIR spectra of (a) MMA, (b) DMAEMA, (c) PMMA-Br, and (d) PMMA-*b*-PDMAEMA.

copolymer PMMA-*b*-PDMAEMA was obtained after polymerization at 90°C for 12 h. Figure 2 shows the ln([M_0]/[M]) and monomer conversion as a function of time for the AGET ATRP of PMMA and PMMA-*b*-PDMAEMA, where [M_0] is the initial monomer concentration and [M] is the monomer concentration.[33] The polymerization shows a linear relationship between the ln([M_0]/[M]) and time (Figure 2), and first-order kinetics was obtained, indicating that the polymer chain growth was consistent with a controlled process. The propagating free-radical concentration remains constant during the polymerization and the termination reactions could be neglected.

FTIR and ^{1}H NMR Spectroscopy. The FTIR spectra of monomer MMA, DMAEMA, PMMA, and PMMA-*b*-PDMAEMA are shown in Figure 3. In Figure 3(a), the absorption bands at 2951 and 1730 cm^{-1} correspond to the C—H stretching of methyl groups and carbonyl group of MMA. Compared with the spectrum of monomer MMA, the characteristic band at 1650 cm^{-1} representing the stretching vibration of C=C disappears in PMMA [Figure 3(c)], which indicates that the monomer MMA have completed the polymerization reaction. In the FTIR spectrum of the amphiphilic block copolymer PMMA-*b*-PDMAEMA [Figure 3(d)], the characteristic band at 1650 cm^{-1} representing the stretching vibration of C=C in DMAEMA disappears. The bands at 1726 cm^{-1} representing C=O and at 2820 and 2760 cm^{-1} representing C—H close to the nitrogen atom stretching for DMAEMA units in the block polymer are also clearly visible.[34] Moreover, the intensity of the C—H stretching vibration at 2951 cm^{-1} decreases on increasing PDMAEMA block length, which indicates that the PDMAEMA has been grafted on the macroinitiators PMMA-Br and forms the amphiphilic block copolymer PMMA-*b*-PDMAEMA.

The chain ends of the PMMA and PMMA-*b*-PDMAEMA polymers synthesized in the presence of air were analyzed by ^{1}H NMR spectroscopy (Figure 4). The chemical shift at δ 4.14 ppm [c in Figure 4(a)] can be attributed to the methylene protons of the ethyl ester unit in the initiator EBiB, indicating that the

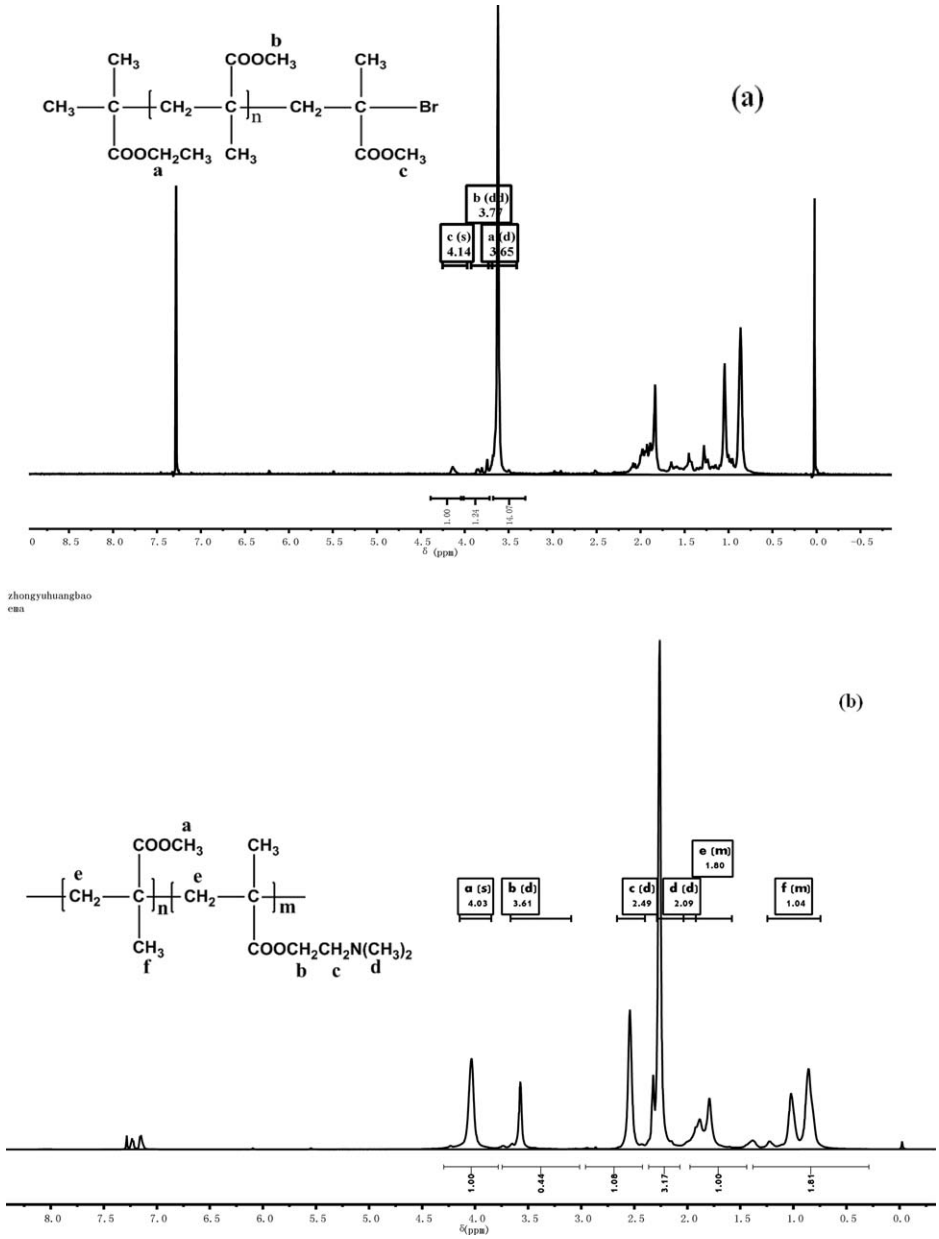

Figure 4. ^{1}H NMR spectra of (a) PMMA and (b) PMMA-*b*-DMAEMA obtained by AGET ATRP with $CDCl_3$ as solvent and TMS as internal standard.

initiator EBiB moieties are successfully attached to the polymer chain ends. The chemical shift at δ 3.77 ppm [b in Figure 4(a)] corresponds to the methyl ester group at the chain end, which deviates from the chemical shift [a, 3.65 ppm, in Figure 4(a)] of the other methyl ester group in PMMA because of the electron-attracting nature of x-Br atom.[35,36] Moreover, the chemical shift at 7.26 ppm corresponds to the characteristic peak of the solvent $CDCl_3$.[37] Therefore, the obtained PMMA can be used as the macroinitiator to conduct chain extension reactions.

The ^{1}H NMR in a nonselective solvent ($CDCl_3$) was also carried out to determine the composition of the amphiphilic block copolymer, PMMA-*b*-PDMAEMA, as shown in Figure 4(b). The chemical shift at δ 4.03 ppm due to the methoyloxy protons (a) of PDMAEMA overlaps with the signal at δ 3.61 ppm due to the methoyloxy protons (b) for the amphiphilic block copolymers with PMMA. The typical chemical shifts at δ 1.04, 1.8, 2.09, and 2.49 ppm can be attributed to the (f) —CH_3 methyl, (e) —CH_2— methylene, (d) N—CH_3 methyl, and (c) N—CH_2— methylene protons of the PMMA-*b*-PDMAEMA side chains, respectively.[38] The ^{1}H-NMR analysis of PMMA-*b*-PDMAEMA indicates that the PDMAEMA moieties exist in the synthesized copolymer.

GPC Characterization. The number-average molecular weight (M_n) and PDI (M_w/M_n) of PMMA and amphiphilic block copolymer, PMMA-*b*-PDMAEMA, were obtained by GPC analysis, and the results are shown in Figure 5. It shows that the M_n values of PMMA and PMMA-*b*-PDMAEMA are 1,1200 and 2,3700 g/mol, respectively, indicating that the PDMAEMA has

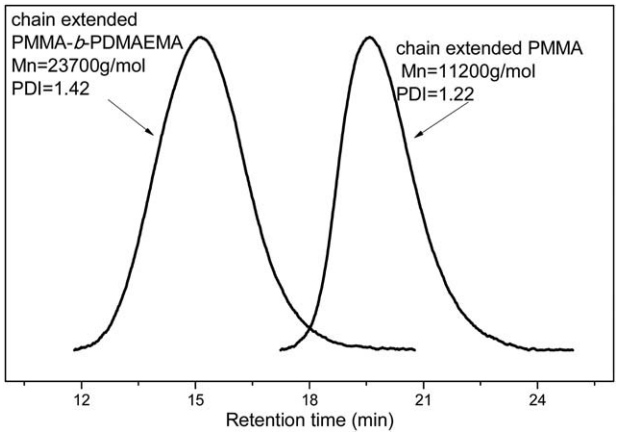

Figure 5. GPC traces of chain extension using PMMA and PMMA-*b*-PDMAEMA prepared by AGET ATRP.

been successfully blocked on the PMMA by AGET ATRP. The PMMA ($M_w/M_n = 1.22$) and PMMA-*b*-PDMAEMA ($M_w/M_n = 1.42$) show low-molecular-weight distributions. The successful chain extension further verifies the advantages of the controlled/"living" free-radical polymerization of PMMA and PMMA-*b*-PDMAEMA using this catalyst system in the presence of a limited amount of air.

Morphologies of Pure PVDF and PVDF/PMMA-*b*-PDMAEMA Blend Membranes

As an amphiphilic additive, PMMA-*b*-PDMAEMA plays a significant role in the pore structure development of membranes. The SEM images of both the cross-sections and top surfaces of blend PVDF membranes with different PMMA-*b*-PDMAEMA contents are shown in Figure 6. All the PVDF membranes show the characteristics of asymmetric membranes synthesized by the wet-phase inversion method, consisting of a dense surface layer and a porous sublayer. The magnified image of the upper part of the blend membrane structure show that the thickness of the skin layer decreases and the number of pores increases with the increase of PMMA-*b*-PDMAEMA content in the casting solution. Compared to those in the pure membrane, the finger-like pores in the sublayer of the blend membrane are smaller in size, but exist in large quantities. The finger-like pore structure developed across the entire cross-sections of the membranes, thus affecting the permeability properties of the blend membranes. The evolutions found in the surfaces and cross-sections of the membranes confirm that the block copolymers are capable of increasing the solvent–nonsolvent exchange, thus acting as a novel porogen. During the exchange of casting solvent (DMAc) and nonsolvent (the water in coagulation bath) in the phase inversion process, the hydrophilic PDMAEMA segregates toward the top surface of the just-formed membrane, and PMMA hinders the leaching of PVDF segments from the as-synthesized membrane. Apparently, the block copolymer significantly affects the membrane formation process. As the membrane skin layer is formed within a very short period of time, the presence of PMMA-*b*-PDMAEMA component in the casting solution may increase the affinity of the casting solution and precipitant. Therefore, the diffusion rate of the solvent and nonsolvent during the phase separation prompts a rapid entry of the polymer solution into the liquid–liquid demixing gap where phase separation takes place.[39] The polymer precipitates rapidly at the interface of solvent and nonsolvent, forming the thinner skin layer.

Moreover, the viscosity of the casting solutions increases with the increase in the amount of the block copolymer in the blend membranes. The increase in the viscosity of the casting solution retards the diffusion rate of the nonsolvent, and the phase separation process becomes a delayed demixing process, thus suppressing the macrovoids in the sublayer. Consequently, the size of the macrovoids in the sublayer becomes smaller. This result is in contrast with those reported by Li,[16] who found that the size of the macrovoids became larger after the addition of amphiphilic comb-shaped copolymer, styrene-(*N*-(4-hydroxyphenyl) maleimide) (SHMI)-*g*-poly (ethylene glycol) methyl ether methacrylate (PEGMA), into the PVDF casting solution. It is presumed that presence of the comb-shaped copolymer SHMI-*g*-PEGMA is more favorable for the formation of the macroviods in the sublayer.

Hydrophilicity of PVDF/PMMA-*b*-PDMAEMA Blend Membranes

Surface hydrophilicity is one of the most important factors to improve the antifouling property of the filtration membranes. Usually, water contact angle measurement is the most convenient method to obtain the relative hydrophilicity of a polymer membrane surface. Figure 7 shows the static water contact angle measurements of the blend membrane as a function of PMMA-*b*-PDMAEMA content in the membrane. The result indicates that the contact angle of the blend membranes decreases significantly with the increase in the PMMA-*b*-PDMAEMA content in the membrane. The contact angle from pristine PVDF membrane 98° decreases to 75° with 15 wt % PMMA-*b*-PDMAEMA incorporation into the blend membrane, which indicates that the incorporation of PMMA-*b*-PDMAEMA is favorable to the surface hydrophilicity of the blend membrane.

Time-dependent contact angle measurement is an accepted way to investigate the membrane surface hydrophilicity. Figure 8 shows the time-dependent contact angles of PVDF/PDMAEMA and PVDF/PMMA-*b*-PDMAEMA blend membranes with 12 wt % PDMAEMA or PMMA-*b*-PDMAEMA in the membrane. The contact angle of PVDF/PMMA-*b*-PDMAEMA blend membrane remains stable after decreasing for a short period during the 20 days continuous operation. In contrast, the contact angle of PVDF/PDMAEMA blend membrane increases gradually within the measurement period (Figure 8). The main reason is that the water-soluble linear polymer PDMAEMA in the membranes is easily washed out of the membranes during its application. However, the block copolymers improve the reservation of additives, and the contact angle of PVDF/PMMA-*b*-PDMAEMA blend membrane remains low. The above experimental results indicate that the loss of hydrophilic polymers significantly affects the stability of the blend membrane.

Water Permeation Flux and BSA Absorption Experiments

Water permeation flux and protein absorption rate are considered as the two significant property parameters for ultrafiltration membrane in water and wastewater treatment.[40,41] The water

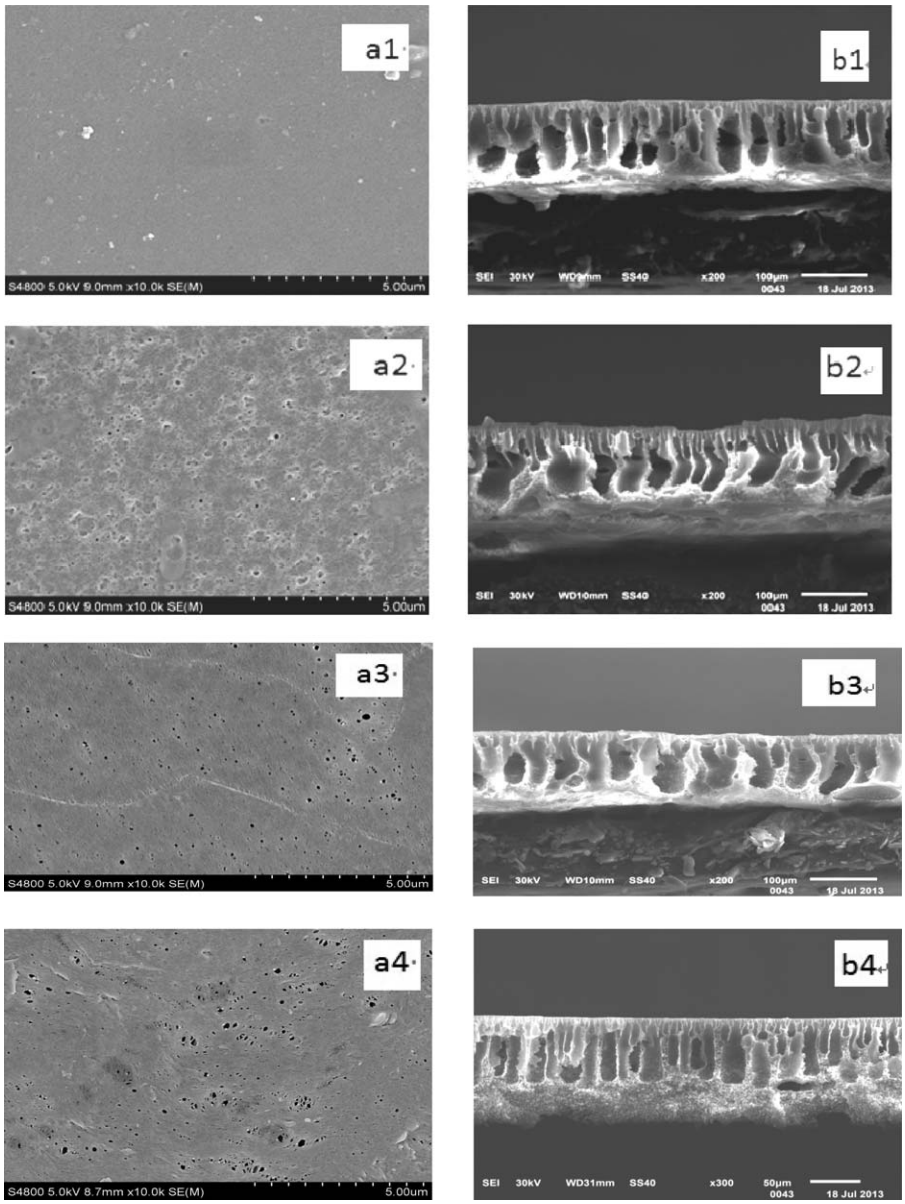

Figure 6. SEM images of the top surface (left) and cross-section (right) of the PVDF blend membrane with 0 wt % (a1 and b1), 5 wt % (a2 and b2), 10 wt % (a3 and b3), and 12 wt % (a4 and b4) PMMA-*b*-PDMAEMA in the blend membrane, respectively.

permeation flux and BSA absorption results of the blend membrane containing different amounts of the block copolymer are shown in Figure 9. The water permeation flux increases with the increase in the PMMA-*b*-PDMAEMA content in the blend membrane up to the maximum value of 122 L/(m^2h) with 15 wt % PMMA-*b*-PDMAEMA incorporation into the membrane. The main reason for the increase in water permeation flux is based on the property of the skin layer of the blend membrane, both the pore size and its porosity, which play a key role in the membrane performance. The SEM images show that the skin layer of the blend membrane becomes thinner after the addition of the block copolymer, contributing to the decrease in the permeation resistance and increase in the pure water flux. Notably, the water flux clearly increases with the increase in the content of PMMA-*b*-PDMAEMA block copolymer in the blend membranes. It can be concluded that the addition of PMMA-*b*-PDMAEMA significantly influences the structure of the blend membranes, thus improving their water flux.

To evaluate the antifouling property of the modified membranes, the protein adsorption of the membrane was measured after immersing the sample in a solution of 0.1 wt % BSA for 24 h. The positive effect of the hydrophilicity enhancement on the antifouling ability of the membrane via a reduction of the protein adsorption had been reported in the Ref. 42. From Figure 9, it can be seen that the high BSA adsorption on a pristine PVDF membrane of 111 ± 3 g/cm^2 slightly reduces to 101 ± 2 g/cm^2 with 5 wt % PMMA-*b*-PDMAEMA in the blend membrane. Such a behavior can be explained by a slight improvement in the material wettability by water. The BSA

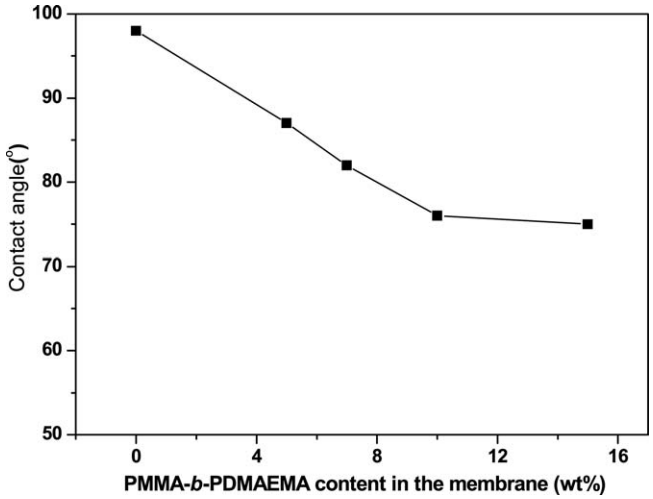

Figure 7. Effect of block copolymer content on the water contact angle of the blend membrane.

adsorbed amount decreases to 46 ± 2 g/cm^2 with 15 wt % PMMA-*b*-PDMAEMA in the blend membrane, indicating that the decrease in protein adsorption amount of the blend membranes is more significant at a higher block copolymer loading. The decrease in the protein adsorption of the blend membranes with the increase in the amount of PMMA-*b*-PDMAEMA indicates that the block copolymer in the membrane improves the general antifouling ability of the PVDF membranes.

Cleaning Experiment of the Blend Membranes. To investigate the fouling resistance of the prepared blend membranes, after testing the pure water flux, BSA used as a model protein solution permeation process was conducted in this study. After that, the membranes were cleaned and pure water fluxes were measured again.[16] The water flux reduction ratio (FR) and the reversible fouling index (RFI) are list in the Table II. As observed, the FR and RFI of the pristine PVDF membrane is 33.9% and 0.879, respectively, because of the hydrophobic property of PVDF material. With the increase of the block copolymer content in the blend membranes, the FR and RFI of the PVDF blend membrane decrease. The FR and RFI of the membrane decrease to 23.3% and 0.716, respectively, with 15 wt % PMMA-*b*-PDMAEMA incorporation into the blend membrane. This can be attributed to the fact that the enrichment of the amphiphilic polymer PMMA-*b*-PDMAEMA in the blend membrane increases the hydrophilicity of the membrane surface. Therefore, the protein molecules have little or no conformational change when they approach the membrane surface, and the reversible protein adsorption or deposition decreases dramatically. As a result, a reduced FR and RFI are obtained and the antifouling property of the blend membrane increases.

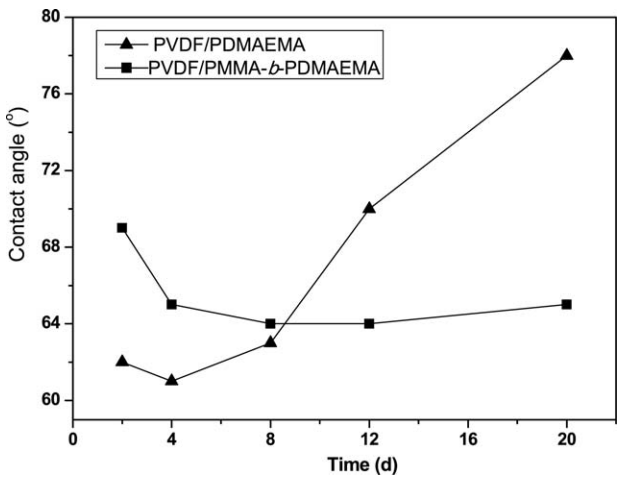

Figure 8. Hydropholicity stability test results of the PVDF/PDMAEMA and PVDF/PMMA-*b*-PDMAEMA blend membrane (the PDMAEMA or PMMA-*b*-PDMAEMA content of 12 wt % in the blend membrane).

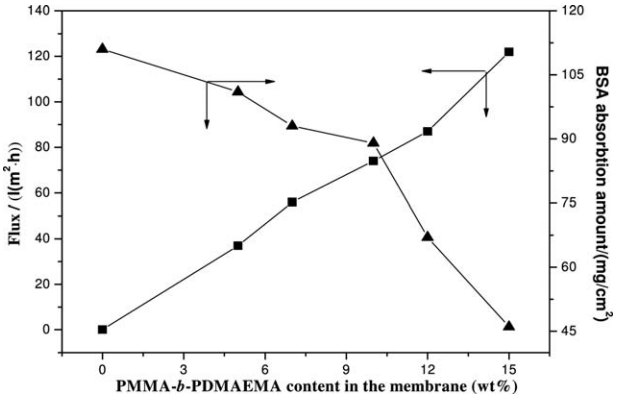

Figure 9. Pure water flux and BSA absorption of the blend membrane as a function of PMMA-*b*-PDMAEMA concentration.

CONCLUSIONS

The amphiphilic block copolymers, PMMA-*b*-PDMAEMA, were synthesized by AGET ATRP using well-defined PMMA-Br as the macroinitiator. The GPC results indicate that the molecular weight distributions of the block copolymers were fairly narrow, confirming the controlled/"living" radical polymerization by the AGET ATRP technology. Then, PVDF/PMMA-*b*-PDMAEMA blend membranes were prepared by the immersion precipitation phase inversion process using the synthesized PMMA-*b*-PDMAEMA as the additive. The SEM images showed that the formation of large macrovoids was suppressed in the blend membrane after incorporation the block copolymer. The magnified images of the upper part of the cross-section of the blend membrane structure showed that the increase in the PMMA-*b*-PDMAEMA content in the casting solution decreased the

Table II. Water Flux Reduction (*FR*) and Reversible Fouling Index (RFI) of PVDF Blend Membranes Containing Difference PMMA-*b*-PDMAEMA Content

Membrane	FR (%)	RFI
Pure PVDF	33.9	0.879
5 wt % M-D/PVDF	31.7	0.827
7 wt % M-D/PVDF	29.6	0.799
10 wt % M-D/PVDF	27.3	0.758
12 wt % M-D/PVDF	24.8	0.734
15 wt % M-D/PVDF	23.3	0.716

thickness of the skin layer and increased the porosity. Over the 20 days continuous operation, the contact angle of the blend membranes almost remained unchangeable, confirming that the hydrophilicity of the blend membrane was stable. The water flux and BSA absorption experiments indicated that the anti-fouling performance of blend membranes was improved by the introduction of an appropriate amount of PMMA-*b*-PDMAEMA into the membranes. The results indicate that PMMA-*b*-PDMAEMA affected the structure of the membranes and improved the hydrophilicity and antifouling characteristics of the PVDF membrane after adding the amphiphilic block copolymers PMMA-*b*-PDMAEMA.

ACKNOWLEDGMENTS

The authors gratefully acknowledge the financial support from the National Natural Science Foundation of China (Grant No. 21406268), the Shandong Provincial Natural Science Foundation (No. ZR2014BM005) and the Fundamental Research Funds for the Central Universities (Grant No. 14CX05034A).

REFERENCES

1. Fukada, E. *Ultrason. Ferroelectr. Freq. Control.* **2000**, *47*, 1277.
2. Khayet, M.; Feng, C. Y.; Khulbe, K. C.; Matsuura, T. *Polymer* **2002**, *43*, 3879.
3. Zhang, B.; Ma, S. *Modern Appl. Sci.* **2009**, *3*, 52.
4. Liu, F.; Hashim, N. A.; Liu, Y.; Abed, M. R. M.; Li, K. *J. Membr. Sci.* **2011**, *375*, 1.
5. Sun, W.; Liu, J.; Chu, H.; Dong, B. *Membranes* **2013**, *3*, 226.
6. Du, J. R.; Peldszus, S.; Huck, P. M.; Feng, X. *Water Res.* **2009**, *43*, 4559.
7. Kato, K.; Uchida, E.; Kang, E. T.; Uyama, Y.; Ikada, Y. *Prog. Polym. Sci.* **2003**, *28*, 209.
8. Zhou, Q.; Lei, X. P.; Li, J. H.; Yan, B. F.; Zhang, Q. Q. *Desalination* **2014**, *337*, 6.
9. Botelho, G.; Silva, M. M.; Goncalves, A. M.; Sencadas, V.; Serrado-Nunes, J.; Lanceros-Mendez, S. *Polym. Test.* **2008**, *27*, 818.
10. Yuan, Z.; Dan-Li, X. *Desalination* **2008**, *223*, 438.
11. Zhao, Y. H.; Zhu, B. K.; Kong, L.; Xu, Y. Y. *Langmuir* **2007**, *23*, 5779.
12. Rajabi, H.; Ghaemi, N.; Madaeni, S. S.; Daraei, P.; Khadivi, M. A.; Falsafi, M. *Appl. Surf. Sci.* **2014**, *313*, 207.
13. Li, X.; Pang, R.; Li, J.; Sun, X.; Shen, J.; Han, W.; Wang, L. *Desalination* **2013**, *324*, 48.
14. Zhu, Y.; Wang, D.; Jiang, L.; Jin, J. *NPG Asia Mater.* **2014**, *6*, e101.
15. Hester, J. F.; Banerjee, P.; Mayes, A. M. *Macromolecules* **1999**, *32*, 1643.
16. Li, J.; Xu, Y.; Wang, J.; Du, C. *Chin. J. Polym. Sci.* **2009**, *27*, 821.
17. Zhao, Y.; Qian, Y.; Zhu, B.; Xu, Y. *J. Membr. Sci.* **2008**, *310*, 567.
18. Kato, M.; Kamigaito, M.; Sawamoto, M.; Higashimura, T. *Macromolecules* **1995**, *28*, 1721.
19. Percec, V.; Barboiu, B. *Macromolecules* **1995**, *28*, 7970.
20. Delaittre, G.; Rieger, J.; Charleux, B. *Macromolecules* **2011**, *44*, 462.
21. Even, M.; Haddleton, D.; Kukulj, D. *Eur. Polym. J.* **2003**, *39*, 633.
22. Wayland, B. B.; Basickes, L.; Mukerjee, S.; Wei, M. L. *Macromolecules* **1997**, *30*, 8109.
23. Peng, H.; Cheng, S.; Fan, Z. *Polym. Eng. Sci.* **2005**, *45*, 1508.
24. Ishio, M.; Terashima, T.; Ouchi, M.; Sawamoto, M. *Macromolecules* **2010**, *43*, 920.
25. Bai, L.; Zhang, L.; Cheng, Z.; Zhu, X. *Polym. Chem.* **2012**, *3*, 2685.
26. Hu, Z.; Shen, X.; Qiu, H.; Lai, G.; Wu, J.; Li, W. *Eur. Polym. J.* **2009**, *45*, 2313.
27. Meng, J. Q.; Chen, C. L.; Huang, L. P.; Du, Q. Y.; Zhang, Y. F. *Appl. Surf. Sci.* **2011**, *257*, 6282.
28. Liu, C. H.; Pan, C. Y. *Polym. Chem.* **2011**, *2*, 563.
29. Kwak, Y.; Magenau, A. J. D.; Matyjaszewski, K. *Macromolecules* **2011**, *44*, 811.
30. Chan, N.; Cunningham, M. F.; Hutchinson, R. A. *Macromol. Chem. Phys.* **2008**, *209*, 1797.
31. Bradford, M. *Anal. Biochem.* **1976**, *72*, 248.
32. Abbasi, M.; Taheri, A. *Indian J. Chem. Technol.* **2014**, *21*, 49.
33. Jakubowski, W.; Min, K.; Matyjaszewski, K. *Macromolecules* **2006**, *39*, 39.
34. Jin, L.; Deng, Y.; Hu, J.; Wang, C. *J. Polym. Sci. Part A: Polym. Chem.* **2004**, *42*, 6081.
35. Zhang, L.; Cheng, Z.; Shi, S.; Li, Q.; Zhu, X. *Polymer* **2008**, *49*, 3054.
36. Cheng, Z.; Zhu, X.; Chen, G.; Xu, W.; Lu, J. *J. Polym. Sci. Part A: Polym. Chem.* **2002**, *40*, 3823.
37. Farca, A.; Resmerita, A.; Stefanache, A.; Balan, M.; Beilstein, H. V. *J. Org. Chem.* **2012**, *8*, 1505.
38. Xiong, Q.; Ni, P.; Zhang, F.; Yu, Z. *Polym. Bull.* **2004**, *53*, 1.
39. Rahimpour, A.; Madaeni, S. S.; Zereshki, S.; Mansourpanah, Y. *Appl. Surf. Sci.* **2009**, *255*, 7455.
40. Deng, B.; Yu, M.; Yang, X.; Zhang, B.; Li, L.; Xie, L.; Li, J.; Lu, X. *J. Membr. Sci.* **2010**, *350*, 252.
41. Meng, H.; Cheng, Q.; Wang, H.; Li, C. *J. Chem.* **2014**, http://dx.doi.org/10.1155/2014/304972.
42. Zhou, Y.; Wang, Z.; Zhang, Q.; Xi, X.; Zhang, J.; Yang, W. *Desalination* **2012**, *307*, 61.